# Uniform Diffusion of Acetonitrile Inside Carbon Nanotubes Favors Supercapacitor Performance

**ARTICLE** *in* NANO LETTERS · AUGUST 2008

Impact Factor: 13.59 · DOI: 10.1021/nl072976g · Source: PubMed



**4 AUTHORS**, INCLUDING:

Oleg N. Kalugin
V. N. Karazin Kharkiv National University
**74** PUBLICATIONS **398** CITATIONS
SEE PROFILE

Valentin Loskutov
Mari State University
**11** PUBLICATIONS **72** CITATIONS
SEE PROFILE

Oleg Prezhdo
University of Rochester
**306** PUBLICATIONS **6,778** CITATIONS
SEE PROFILE

NANO LETTERS

2008
Vol. 8, No. 8
2126-2130

# Uniform Diffusion of Acetonitrile inside Carbon Nanotubes Favors Supercapacitor Performance

**Oleg N. Kalugin,*,† Vitaly V. Chaban,† Valentin V. Loskutov,‡ and Oleg V. Prezhdo*,§**

*Department of Inorganic Chemistry, Kharkiv National University, Kharkiv, Ukraine, Department of Physics and Mathematics, Mari State Pedagogical Institute, Yoshkar-Ola, Russia, and Department of Chemistry, University of Washington, Seattle, Washington*

*Received November 14, 2007; Revised Manuscript Received May 5, 2008*

## ABSTRACT

**An unusual behavior of liquid acetonitrile (AN) confined inside carbon nanotubes (CNTs) is predicted by molecular dynamics simulation. In contrast to water, which shows inhomogeneous variation of both translational and rotational diffusion with CNT diameter [*Nano Lett.* 2003, *3*, 589; 2004, *4*, 619], the diffusion coefficient of AN changes uniformly and can be described by a simple analytic model. At the same time, the reorientation dynamics of AN vary irregularly in smaller CNTs because of specific packing structures. The uniform translational diffusion of the nonaqueous solvent is critical for stable performance of the new generation of supercapacitors [*Nat. Mater.* 2006, *5*, 987].**

Molecular motions inside carbon nanotubes (CNTs) attract great attention due to the unique properties of liquids and gases in the confined environments,[1–10] motivating a variety of novel applications based on these unique properties.[11–15] Thus, water confined inside CNTs is drastically different from bulk water and can undergo a transition to a new state with ice-like mobility but liquid-like hydrogen bonding.[2,4,7,8] *N*-alkanes in CNTs exhibit capillary phase transitions, involving stable, metastable, and unstable regimes.[5,16] CNTs provide an excellent model for studying ionic transport through hydrophobic channels, which are ubiquitous in biological membranes. Such studies elucidate the differences between anionic and cationic transport and reveal liquid−vapor oscillations resulting in anomalously high molecular mobilities.[1,3,6,17,18] Insertion and translocation of molecules through CNTs form the basis for many new devices, including efficient nanofluidic channels,[12,15] molecular convergent nozzles,[13] and vapor sensors.[14]

Particularly interesting and promising are applications of CNTs as electrode materials. Nanoporous carbon exhibits excellent charge−discharge properties and a stable cyclic life. Moreover, activated composite carbon films generate high specific capacitance, laying the foundation for a new generation of double-layer supercapacitors (SC).[11,19–21] CNTs provide an ideal model for investigating the microscopic details of fluid transport in these nanoporous carbon structures. SC design requires polar but aprotic solvents such as acetonitrile (AN). AN's structural, transport, and solvation characteristics are notably different from those of polar, protic liquids such as water and alcohols[2,4,7,8,22,23] on the one hand, and nonpolar, aprotic liquids such as alkanes[5,16] on the other hand. In spite of the great fundamental and practical importance of AN, its structural and dynamical properties inside CNTs have not been investigated yet.

The current letter reports the first atomistic simulations of structure and mobility of AN confined inside CNTs of varying radii. We find that CNTs impose strong cylindrical anisotropy in the structure of liquid AN, reminiscent of the solid state. Both translational and rotational dynamics are slowed down by the geometric confinement. In contrast to water, which shows a nonlinear dependence of the diffusion coefficient on the CNT diameter,[2] the diffusion coefficient of AN is a uniform function of the CNT size. In order to represent this straightforward behavior, we derive a simple physical model that successfully extrapolates the CNT data to the bulk result. At the same time, the reorientation dynamics of AN molecules exhibit anomalies associated with specific solvent structures inside smaller CNTs. In some cases, molecular confinement favors tightly packed structures, while in other cases AN molecules are allowed extra free space. This irregular behavior is reminiscent of the liquid−vapor oscillations seen with hydrated $K^+$ ions in bacterial channels,[6] and the stable, metastable, and unstable regimes in *n*-alkanes inside CNTs.[5] Judging by the intuition gathered from the

* Corresponding authors. E-mail: Oleg.N.Kalugin@univer.kharkov.ua (O.N.K.) and prezhdo@u.washington.edu (O.V.P.).
† Kharkiv National University.
‡ Mari State Pedagogical Institute.
§ University of Washington.

10.1021/nl072976g CCC: $40.75 
**Published on Web 07/16/2008**

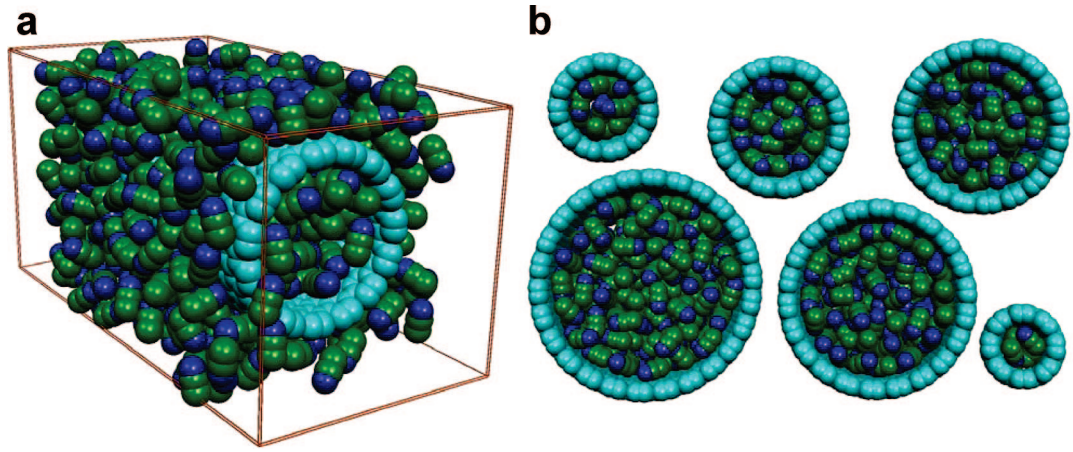


**Figure 1.** Snapshots of MD simulation cells from simulations of AN confined inside CNTs at 298 K; see Table 1. (a) Simulation cell of the (15 × 15) CNT system. (b) Side view of all systems, omitting AN molecules outside CNTs.

**Table 1.** System Parameters and Dynamic Properties of AN Molecules Confined Inside CNTs

| system | CNT internal diameter, $d_{CNT}$, (nm) | CNT length, $L_{CNT}$, (nm) | number of carbon atoms in CNT | AN self-diffusion coefficient, $D{\cdot}10^9$, ($m^2/s$) | AN orientation relaxation time, $\tau_\mu$, (ps) |
|---|---|---|---|---|---|
| 216 AN (bulk) | | | | 3.240 ± 0.004 | 3.9 |
| 216 AN + (8,8) CNT | 0.707 | 3.074 | 288 | 0.76 ± 0.07 | 18.1 |
| 281 AN + (11,11) CNT | 1.113 | 3.074 | 572 | 1.09 ± 0.22 | 102 |
| 432 AN + (15,15) CNT | 1.655 | 4.058 | 1020 | 1.69 ± 0.12 | 11.9 |
| 608 AN + (19,19) CNT | 2.197 | 5.042 | 1596 | 2.03 ± 0.12 | 9.1 |
| 887 AN + (22,22) CNT | 2.604 | 6.026 | 2200 | 2.27 ± 0.05 | 9.0 |
| 1530 AN + (26,26) CNT | 3.526 | 7.010 | 3016 | 2.52 ± 0.05 | 7.9 |

water−CNT simulations,[1,2,4,7,8,10,18,24] the different effects of the solvent confinement on the translational and rotational dynamics are rather unexpected. The fact that translational diffusion varies uniformly with the CNT diameter is very positive for SC applications, since it ensures continuous and stable SC performance for different manufacturing and operation regimes.

The simulations were performed on a set of six systems containing armchair CNTs of different diameter and length immersed in liquid AN of bulk density at 298 K, Table 1. For reference, the corresponding properties of bulk AN were calculated as well. The simulations were carried out using the proprietary software package MDCNT (molecular dynamics inside carbon nanotubes)[21] with periodic boundary conditions in all directions. Open-ended CNTs were located in the parallelepiped cell and were surrounded by a few layers of AN molecules, Figure 1. The molecules were free to migrate in and out of the CNTs. AN was described by the three-site rigid A3 model,[25] with the site−site intermolecular interactions represented by the sum of the Lennard-Jones (LJ) shifted-force potential and the Coulomb potential with reaction-field modification. A rotational analog of the Verlet algorithm was used for the rigid AN molecules.[26] The force field of the CNT carbon atoms was taken to be purely LJ, with the potential parameters $\sigma = 0.33611$ nm and $\varepsilon = 0.405868$ kJ/mol.[27]

The MD simulations of all of the systems were performed with a 1 fs time step, in the NVT ensemble, and at 298 K using Berendsen thermostat with the relaxation time of 100 fs. The carbon atoms of the CNTs were held fixed during the MD simulations. System equilibrations were performed over 200 ps, and the data were collected over at least 5 runs of 500 ps duration each.

The solvent structure of AN inside CNTs was analyzed by computing the cylindrical distribution function $g_{\alpha\beta}(z,r)$ of the atomic density along the CNT axial ($z$) and radial ($r$) directions. Figure 2 shows two examples of the distributions of nitrogen atomic density of AN molecules confined inside the (15,15) and (19,19) armchair CNTs with the internal diameters of 1.655 and 2.197 nm, respectively. The same oscillatory behavior of the atomic density along the radial direction was observed for all CNTs and all AN interacting sites, including N, C, and $CH_3$. The atomic density is maximal near the CNT wall, where molecular correlations are reinforced by the space confinement. The second maximum in the atomic density is seen about 0.35 nm after the first maximum. The height of the second maximum is ~1.5 times smaller than the height of the first maximum. This trend was seen in all cases. At distances larger than 0.7 nm from the CNT wall, the confinement effects can be neglected.

One can expect that the spatial confinement of the AN molecules at distances shorter than 0.7 nm from the CNT wall should have an important impact on the solvent dynamical and transport properties. The confinement effect is seen with both the reorientation dynamics and the diffusion coefficient. These types of motion are slowed down inside CNTs. The diffusion shows a uniform dependence on the CNT diameter, while the reorientation exhibits strong anomalies in the CNTs whose radii are less than 0.7 nm, as elucidated below.

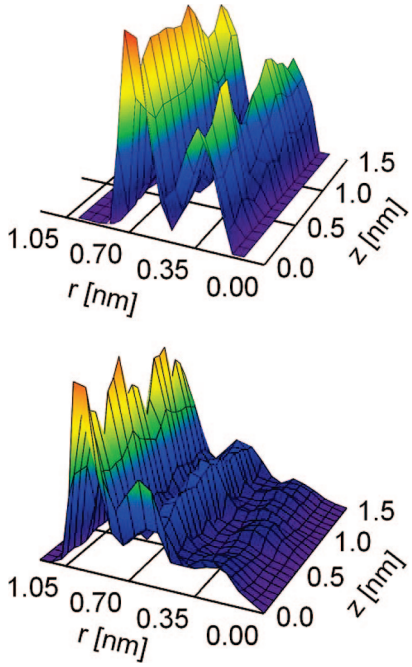


**Figure 2.** Cylindrical distribution functions of nitrogen atom density inside (15,15) and (19,19) CNTs, top and bottom panels, respectively.

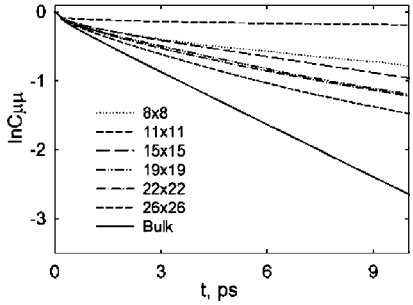


**Figure 3.** Logarithms of the orientation ACFs vs time for AN molecules in bulk solvent and inside CNTs.

In order to examine the orientation dynamics of the AN molecules inside CNTs, we evaluated the orientation autocorrelation function (ACF) of the unit vector **u** along the direction of the molecular dipole $\mu$, $C_{\mu\mu}(t) = \langle \mathbf{u}(0)\cdot\mathbf{u}(t)\rangle / \langle \mathbf{u}(0)\cdot\mathbf{u}(0)\rangle$. The logarithms of these ACFs versus time are shown in Figure 3. The long-time behavior of $C_{\mu\mu}(t)$ extending beyond 2 ps is well-described by a single exponential decay: $\ln C_{\mu\mu}(t) = \text{const} - t/\tau_\mu$. The corresponding orientation relaxation times, $\tau_\mu$, calculated using the least-squares method from the slopes of $\ln C_{\mu\mu}(t)$ at times between 2 and 10 ps are summarized in Table 1. The reorientation dynamics of AN molecules inside CNTs is drastically slower than that in bulk liquid. The orientation relaxation times significantly exceed the bulk value and increase with decreasing CNT diameter. A uniform behavior is seen with the nanotubes from (26,26) to (11,11), whose diameters are more than twice larger than the 0.7 nm confinement distance, discussed above. The orientation relaxation time of AN inside the (11,11) CNT, whose diameter is 1.1 nm, jumps to an extremely large value of 102 ps. Surprisingly, the relaxation time for the (8,8) time with internal diameter of only 0.7 nm is quite small, $\tau_\mu = 18.1$ ps, and is much closer to that of the (15,15) tube, $\tau_\mu = 11.9$ ps, than the (11,11) tube, even though the spatial confinement effects should be strongest in the (8,8) CNT.

The unexpected behavior seen with the solvent reorientation dynamics in the smallest CNTs can be rationalized by considering the packing of the AN molecules inside the (8,8) and (11,11) tubes, Figure 4. In both cases, spatial confinement affects all solvent molecules inside the tubes, since the CNT radius is less than the 0.7 nm confinement length. The density of solvent molecules is rather low in the (8,8) tube, because of the weak interaction between the polar AN and the nonpolar CNT. The AN molecules form a single cylindrical shell inside the tube and are located relatively far away from the tube wall. The low solvent density, weak AN-CNT interaction, and large distance between the AN molecules and the CNT wall result in a relatively rapid reorientation dynamics. The situation is quite different for the (11,11) CNT, which accommodates not only the cylindrical shell of AN molecules, but also an extra string of molecules close to the CNT axis, Figure 4. This allows for significantly better solvent−solvent interactions and, therefore, a higher solvent density inside the tube. The extra string of AN molecules pushes the shell molecules close to the CNT wall, impeding the orientation dynamics. The changes in the orientation relaxation time as a function of the CNT diameter, Table 1, can be understood by considering the fraction of solvent molecules immediately adjacent to the CNT wall relative to those surrounded by other molecules. Translational diffusion of AN inside CNTs is of great importance to a variety of applications.[11–15,20] The self-diffusion coefficient $D$ was calculated by the Green-Kubo formula

$$D = \frac{1}{3}\int_0^\infty C_{vv}(t)dt \qquad (1)$$

in which $C_{vv}(t)$ is the autocorrelation function of the center-of-mass translational velocity. In order to avoid the open-end boundary effects, only AN molecules located more than one molecule diameter (0.6 nm) away from the nanotube ends were used to calculate $D$. The values reported in Table 1 clearly show that the diffusion coefficient of AN inside CNTs decreases with decreasing CNT diameter. The change between bulk and the 1 nm (8,8) CNT is a factor of 4. The behavior of the translational diffusion coefficient is uniform, in contrast to the corresponding variation in the orientation relaxation time, Table 1. This result is very important for such practical applications as double-layer SC,[11,19–21] which require steady solvent diffusion inside nanoporous carbon of varying pore-diameter distributions. The spatial confinement influences the translational motion to a lesser extent than the rotational motion, as follows from data reported in Table 1.

Optimization and development of electrochemical devices based on nanoporous carbon requires an analytic expression for the self-diffusion coefficient of a liquid inside the nanopores of arbitrary diameter and length. In the absence of a general theory of fluid diffusion in porous materials, we extended the recently proposed description of liquid transport under steric confinement of a solid matrix[28] and obtained a simple analytic expression for the observed trend in the diffusion coefficient, as described below.

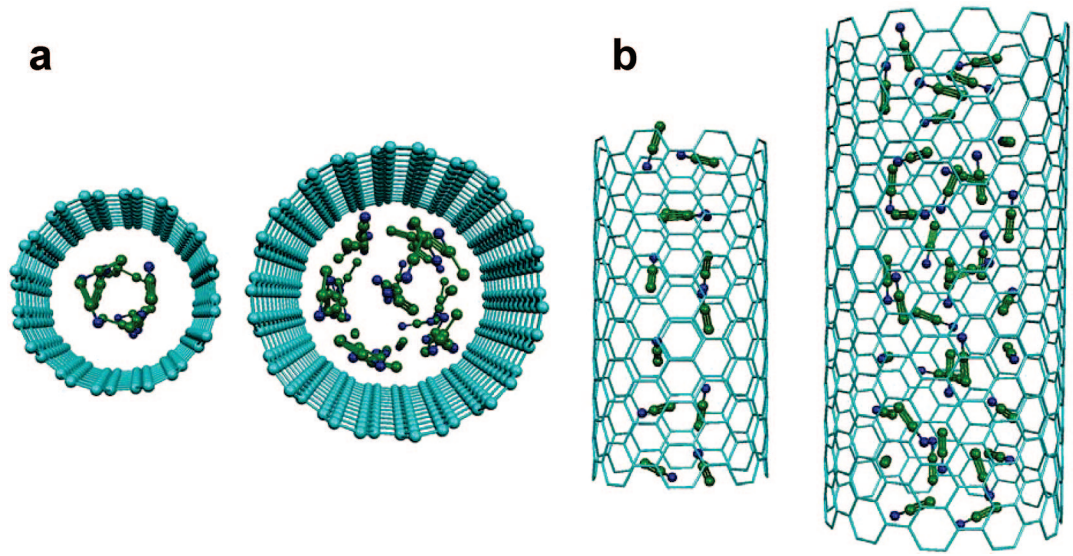


**Figure 4.** (a) Side and (b) top views of AN confined inside (8,8) and (11,11) CNTs, which show anomalous AN reorientation times; see Table 1.

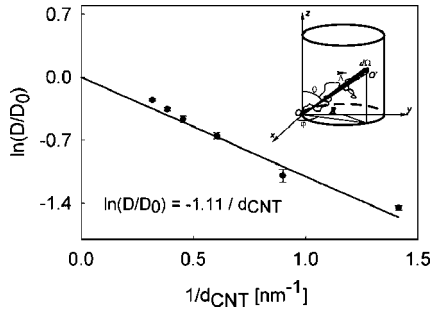


**Figure 5.** Relative AN diffusion coefficient as a function of CNT inverse diameter. Inset: Diffusion path of a particle inside a CNT.

Reference 28 shows that self-diffusion of a liquid in a heterogeneous system is decreased relative to the pure liquid according to

$$D = D_0 \exp(-P_{st}) \tag{2}$$

where $D_0$ is the bulk self-diffusion coefficient and $P_{st}$ is the probability of steric restrictions imposed on a particle of a fluid by the surrounding matrix. The probability $P_{st}$ is determined by the space distribution of these steric constrains or, in the simplest case, by the confinement geometry.

Consider a liquid molecule that diffuses distance $\Lambda$ and collides with a CNT wall; see insert in Figure 5. Collisions occur when the molecule is close to the CNT wall and moves toward the wall. The thickness of the solvent layer that is sufficiently close to the wall to produce a collision can be estimated by the mean-free path of diffusion $d_m$. The directionality of the molecular motion is accounted for by the following average

$$\langle\Lambda\rangle = \int \Lambda d\Omega / \int d\Omega \tag{3}$$

in which the integration is performed over the solid angle that is directed toward the CNT wall. Geometric considerations lead to

$$\langle\Lambda\rangle \approx 0.64d \tag{4}$$

where $d$ is the internal diameter of the CNT. The probability that the motion of the diffusing particle will be impeded by a collision with the wall is given by the ratio $d_m/\langle\Lambda\rangle$. Then, the expression (2) for self-diffusion coefficient in the confined geometry becomes

$$D = D_0 \exp(-d_m/0.64d) \tag{5}$$

or, explicitly inserting the value of the mean-free diffusion path for bulk AN, $d_m = 0.65$ nm:

$$D = D_0 \exp(-1.01/d) \tag{6}$$

Figure 5 demonstrates good agreement between this simple theoretical expression and the results of the MD simulation, given by the filled circles.

To recapitulate, we reported the first simulation of AN confined inside CNTs and elucidated the details of its structure, reorientation dynamics, and translational diffusion. AN is a widely used aprotic solvent presenting an alternative to water, which has been the focus of the majority of the earlier studies. The geometric confinement creates a strong periodic pattern of AN near the CNT wall, with the persistence length of 0.7 nm. The reorientation relaxation time generally increases with decreasing CNT diameter and varies nonlinearly in small CNTs. Remarkably, the AN translational diffusion coefficient changes continuously with the CNT diameter. This is in contrast to water, which shows nonuniform behavior due to hydrogen bonding. The result can be expected to hold for aprotic solvents in general and is described here with a simple analytic model, which can be used in large-scale modeling of electrochemical materials. In particular, AN is the solvent of choice for the new generation of supercapacitors, which promise to revolutionalize energy storage by creating exceptionally compact devices. The uniform dependence of the AN translational diffusion coefficient established in our work ensures stable performance of the supercapacitors regardless of the CNT diameter distribution.

**Acknowledgment.** The authors acknowledge computational support of the Ukrainian−American Laboratory in Computational Chemistry established between Kharkiv, Ukraine and Jackson, MS, U.S.A. The funding was provided in part by grants from the National Science Foundation, CHE-0701517, and Petroleum Research Fund of the American Chemical Society, 46772-AC6.

## References

(1) Hummer, G; Rasaiah, J. C.; Noworyta, J. P. *Nature* **2001**, *414*, 188–190.
(2) Mashl, R. J.; Joseph, S.; Aluru, N. R.; Jakobsson, E. *Nano Lett.* **2003**, *3*, 589–592.
(3) Joseph, S.; Mashl, R. J.; Jakobsson, E.; Aluru, N. R. *Nano Lett.* **2003**, *3*, 1399–1403.
(4) Lee, Y.; Martin, C. D.; Parise, J. B.; Hriljac, J. A.; Vogt, T. *Nano Lett.* **2004**, *4*, 619–621.
(5) Jiang, J. W.; Sandler, S. I.; Smit, B. *Nano Lett.* **2004**, *4*, 241–244.
(6) Saparov, S. M.; Pohl, P. *Proc. Natl. Acad. Sci. U.S.A.* **2004**, *101*, 4805–4809.
(7) Lu, D. Y.; Li, Y.; Rotkin, S. V.; Ravaioli, U.; Schulten, K. *Nano Lett.* **2004**, *4*, 2383–2387.
(8) Byl, O.; Liu, J. C.; Wang, Y.; Yim, W. L.; Johnson, J. K.; Yates, J. T. *J. Am. Chem. Soc.* **2006**, *128*, 12090–12097.
(9) Li, J. Y.; Gong, X. J.; Lu, H. J.; Li, D.; Fang, H. P.; Zhou, R. H. *Proc. Natl. Acad. Sci. U.S.A.* **2007**, *104*, 3687–3692.
(10) Wang, Z. K.; Ci, L. J.; Chen, L.; Nayak, S.; Ajayan, P. M.; Koratkar, N. *Nano Lett.* **2004**, *7*, 697–702.
(11) Service, R. F. *Science* **2006**, *313*, 902.
(12) Xue, Y. Q.; Chen, M. D. *Nature-Nanotech.* **2006**, *17*, 5216–5223.
(13) Hanasaki, I.; Nakatani, A. *Nature-Nanotech.* **2006**, *17*, 2794–2804.
(14) Parikh, K.; Cattanach, K.; Rao, R.; Suh, D. S.; Wu, A. M.; Manohar, S. K. *Sensors and Actuators B-Chem.* **2006**, *113*, 55–63.
(15) Whitby, M.; Quirke, N. *Nature-Nanotech.* **2007**, *2*, 87–94.
(16) Yang, H.; Liu, Y.; Zhang, H.; Li, Z. S. *Polymer* **2006**, *47*, 7607–7610.
(17) Liu, H. M.; Murad, S.; Jameson, C. J. *J. Chem. Phys.* **2006**, *125*, 084713.
(18) Dellago, C.; Hummer, G. *Phys. Rev. Lett.* **2006**, *97*, 245901.
(19) Huang, Q. H.; Wang, X. Y.; Li, J.; Dai, C. L.; Gamboa, S.; Sebastian, P. J. *J. Power Sources* **2007**, *164*, 425–429.
(20) (a) Hu, Y. S. *Nat. Mater.* **2006**, *5*, 713–717. (b) Futaba, D. N. *Nat. Mater.* **2006**, *5*, 987–994.
(21) Kalugin, O. N.; Chaban, V. V.; Kolesnik, Y. V. *Kharkiv University Bulletin* **2006**, *669*, 41–58.
(22) Barthel J.; Gores H. J. Solution Chemistry: A Cutting Edge in Modern Electrochemical Technology. *Chemistry of Nonaqueous Electrolyte Solutions*; Mamontov, G., Popov, A. I., Eds.; VCH: New York, 1994, *Ch. 1.*
(23) Mosyak, A. A.; Prezhdo, O. V; Rossky, P. J. *J. Chem. Phys.* **1998**, *109*, 6390–6395.
(24) Choudhury, N.; Pettitt, B. M. *J. Am. Chem. Soc.* **2007**, *129*, 4847–4852.
(25) Mountain, R. D. *J. Chem. Phys.* **1997**, *107*, 3921–3923.
(26) Kolesnik, Y. V.; Kalugin, O. N.; Volobuev, M. N. *Chem. Phys.* **2001**, *20*, 16–21.
(27) Van Gunsteren, W. F., et al. *The GROMOS 96 Manual and User Guide*; Biomos b. v.: Zurich, Groningen Zurich, Hochschuverlaf AG auder ETH Zurich, 1996.
(28) Sevriugin, V. A.; Loskutov, V. V.; Skirda, V. D. *Colloid J.* **2003**, *65*, 602–605.

NL072976G